

# Double interplay between localized vs. itinerant, ferro- vs. antiferromagnetism in Ge doped FeGa<sub>3</sub>

J. C. Alvarez-Quiceno,<sup>1</sup> M. Cabrera-Baez,<sup>1</sup> J. Munévar,<sup>1,2</sup> H. Micklitz,<sup>2</sup> E. M. Bittar,<sup>2</sup> E. Baggio-Saitovitch,<sup>2</sup> R. A. Ribeiro,<sup>1</sup> G. M. Dalpian,<sup>1,\*</sup> J. M. Osorio-Guillén,<sup>1,3</sup> and M. A. Avila<sup>1,†</sup>

<sup>1</sup>*Centro de Ciências Naturais e Humanas, Universidade Federal do ABC, Santo André, SP, Brazil*

<sup>2</sup>*Centro Brasileiro de Pesquisas Físicas, Rua Dr. Xavier Sigaud 150, Rio de Janeiro, Brazil*

<sup>3</sup>*Instituto de Física, Universidad de Antioquia UdeA, Calle 70 No 52-21, Medellín, Colombia*

A comprehensive investigation on the complex magnetic properties of the FeGa<sub>3-x</sub>Ge<sub>x</sub> system is presented through a combination of Density Functional Theory, <sup>57</sup>Fe Mössbauer spectroscopy and magnetic susceptibility. Spin density diagrams evidence the emergence of localized magnetic moments on the Fe atoms that leads to a majority ferromagnetic response in the samples with increasing Ge concentration, however, the distribution of magnetic moments is strongly dependent on the dopant configurations (which break the single Fe site symmetry) and in certain cases Fe moments aligned antiparallel are found. We discuss the combined theoretical and experimental results in terms of a scenario wherein increasing Ge-doping leads to an evolution from mostly localized moments at small concentrations to a combination of both localized and itinerant moments with different values in the magnetically ordered state ( $0.13 < x < 0.41$ ), which can be described as ferromagnetic with a fragile antiferromagnetic component.

The physics of Fe-based intermetallic semiconductors such as FeSi, FeSb<sub>2</sub> and FeGa<sub>3</sub> can present very unusual phenomena, creating an important playground for the development of condensed matter science. These materials can present properties of strongly correlated electron systems, owing to the presence of the Fe *d* levels, concurrent with semiconducting gaps due to the strong hybridization between the *d* and *s, p* levels. They have been extensively studied mainly for their thermoelectric properties[1][2][3]. However, they are also interesting from fundamental physical aspects[4], still presenting important, unsolved puzzles.

Here we shall address one such open issue, the puzzling magnetic response upon electronic doping of FeGa<sub>3</sub>, one of the few Fe-based materials known to be diamagnetic. This diamagnetism of the pure compound has been assigned to the strong hybridization between the Fe *3d* levels and the Ga *4s* and *4p* levels. Starting from this already unusual state, strikingly different magnetic responses can be observed upon chemical substitutions that lead to doping with holes or electrons[5].

There is much controversy in the literature regarding the most stable magnetic configurations of pure and doped FeGa<sub>3</sub>, as well as on the mechanisms involved. Some works propose an antiferromagnetic ground state for pure and doped FeGa<sub>3</sub> [6, 7], whereas others report a diamagnetic ground state[8, 9]. There are also authors invoking an itinerant origin for the ferromagnetic ground state [10], whereas other reports show a localized nature for the magnetic moments[11, 12], or both [13].

The multitude of different configurations clearly indi-

cates that more studies are necessary in order to unravel the fundamental properties of FeGa<sub>3</sub>. In order to do so, we have performed a joint theoretical and experimental work by using First-principles Density Functional Theory (DFT) calculations, Mössbauer spectroscopy and bulk magnetization techniques on Ge-doped FeGa<sub>3</sub> single crystals, i.e., on electron-doped materials. Our results confirm that, upon doping, the system quickly evolves to a mainly ferromagnetic (FM) ground state. However, the evolution of magnetism with doping is far from trivial. The magnetic moments are not evenly distributed throughout all Fe atoms as expected in an itinerant picture, and at least two different groupings of magnetic moments on the Fe atoms are resolved, that depend on both doping concentration and dopant distribution. Additionally, some distributions do indeed lead to Fe moments aligned antiparallel to the majority FM state. Our results point to an intricate competition between localized *vs.* itinerant, FM *vs.* AFM pictures for the magnetic response in the doped materials, which may lead to the conclusion that almost all of the previous works were providing partially correct but incomplete descriptions of this fascinating system.

A detailed description of the growth methodology, the experimental characterization procedures and the theoretical calculation settings are all provided in the Supplemental Material. In short: high-quality FeGa<sub>3-x</sub>Ge<sub>x</sub> single crystals were grown by the Ga self-flux technique and DC magnetic susceptibility down to  $T = 2$  K was measured on a Quantum Design SQUID-VSM at UFABC; temperature and field dependent <sup>57</sup>Fe Mössbauer spectroscopy experiments were conducted at CBPF; and First-principles DFT calculations were performed as implemented in the VASP code [14, 15].

The simplest way to theoretically model *p*- and *n*-type doping in FeGa<sub>3</sub> is by shifting the Fermi energy of the

\*Electronic address: [gustavo.dalpian@ufabc.edu.br](mailto:gustavo.dalpian@ufabc.edu.br)

†Electronic address: [avila@ufabc.edu.br](mailto:avila@ufabc.edu.br)

system up or down, which will represent the occurrence of electrons in the conduction band or holes in the valence band, respectively. For this specific case the symmetry of the lattice is kept fixed, and the dopants are initially delocalized throughout the entire system. This preliminary approach leads to the observation that hole injection induces similar magnetic moments in all Fe atoms, whereas electron injection induces moments at Fe atoms that are not homogeneously distributed throughout the supercell (see Supplemental Material). Such a distribution difference of moments for holes and electrons is an indication that different magnetic mechanisms may arise for different types of dopants, some being more delocalized (itinerant) and the others being more localized.

After modelling with a preliminary effective doping model, we advance our calculations to an explicit doping approach of  $\text{FeGa}_3$  with Ge atoms ( $\text{FeGa}_{3-x}\text{Ge}_x$ ). This compound adopts a new structure (FeGa<sub>3</sub>-type) consisting of a layered, tetragonal unit cell with a single crystallographic site for Fe (highly relevant to the analyses and discussions that follow) and two inequivalent sites for Ga: Ga1 shares the same plane with Fe and Ga2 occupies its own separate plane (See Supplemental Material). Calculations were performed with several different configurations for the distribution of Ge dopants throughout supercells of appropriate sizes to obtain the desired concentrations. We have also converged different spin configurations for each atomic distribution, including (i) non-spin polarized, (ii) all Fe atoms with parallel spin and (iii) all Fe dimers with antiparallel spins. For all simulated concentrations, the system prefers the parallel spin configuration since they have the lowest energies.

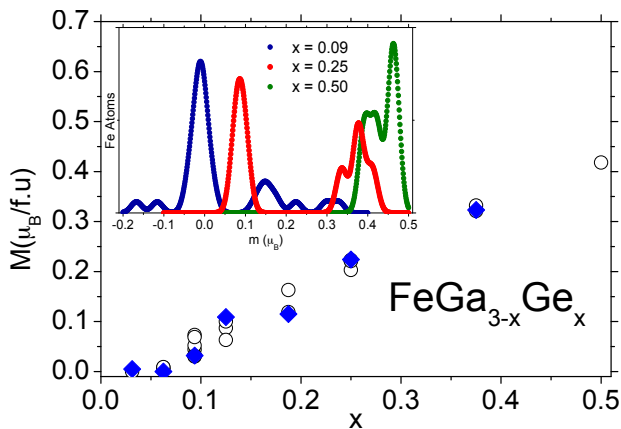


FIG. 1: Total magnetization of  $\text{FeGa}_{3-x}\text{Ge}_x$  per formula unit as a function of Ge atoms concentration  $x$ .

The blue diamonds indicate the lowest energy configuration. Inset: Magnetic moment distribution on the Fe atoms at the lowest energy configurations for  $x = 0.09, 0.25$  and  $0.50$ .

When a single Ge atom is inserted in a  $2 \times 2 \times 2$  supercell at either a Ga1 or Ga2 site ( $x = 0.03$ ), the Ga2 site is

preferred by an energy difference of 0.11 eV. In this case, the Ge atom also induces a small magnetic moment on its Fe neighbors ( $5 \times 10^{-3} \mu_B/\text{f.u.}$ ), whereas at the Ga1 site it does not lead to any magnetic distortion on its vicinity. This contrast demonstrates the complex nature of this material, since the exact lattice position where each Ge atom enters directly influences the magnetic configuration. Consequently, a complete description of the magnetic behavior can only be achieved through a meticulous and thorough exploration involving many different configurations, which we undertake next.

By increasing the dopant concentration in different supercells, we were able to establish several different magnetic configurations, wherein the total moment per unit cell also resulted different. For a given concentration, there can be different spin configurations that differ simply by the distribution of the Ge atoms. This can be observed in Fig. 1, where the total magnetic moment per formula unit is plotted for several different configurations of a certain dopant concentration. The blue dots in this figure indicate the most stable spin configuration. It can be seen that for  $x = 0.03$  and  $0.06$  there are some configurations with null magnetic moment. The inset of Fig. 1 shows the magnetic moment distribution on the Fe atoms for the lowest energy configurations of the  $x = 0.09, 0.25$  and  $0.50$  concentrations (the distributions for all other concentrations are included in the Supplemental Material). The well defined, multiple peaks for each curve indicate that there are distributions around certain values of magnetic moment, rather than a single value for all the Fe atoms. These results clearly pose a question on any calculation performed within the virtual crystal approximation, since through such a method only an average effect can be observed.

With the aim of visualizing the real-space magnetic moment distributions in the system, we plot the calculated spin densities for the more stable distribution of Ge atoms at each concentration (Fig. 2). In these representations one can observe that the induced magnetic moments are initially localized close to the dopant and, increasing the dopant concentration  $x$ , the magnetization gradually spreads throughout the Fe atoms on the lattice, towards a more delocalized character of magnetization at high concentrations. It is also worthy of notice that the lowest energy configurations for  $x = 0.09$  and  $0.19$  exhibit the formation of a few antiparallel spins on the Fe dimers. In all other configurations (including those of larger energy at  $x = 0.09$  and  $0.19$ ) the induced magnetic moments are oriented in the same direction, leading to ferromagnetic states.

Thus, two main points can be derived from the thorough calculations which led to the results in Fig. 2: (I) an initial emergence of localized moments on some Fe atoms nearby diluted Ge impurities evolves, as a function of dopant concentration, into a more delocalised character at larger concentrations, ending in similar moments

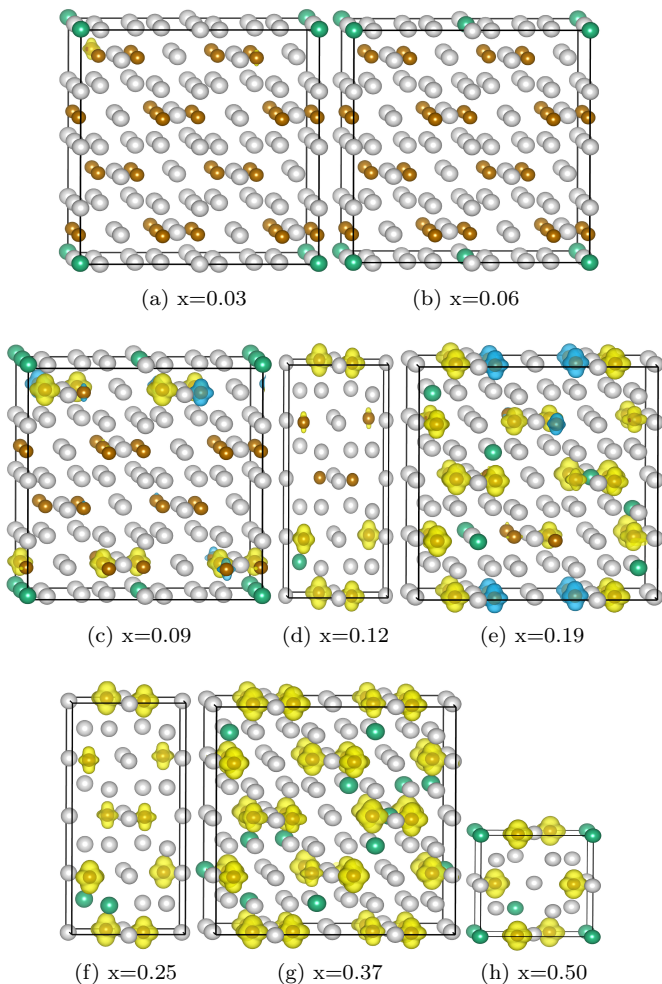


FIG. 2: Spin density distribution for the lowest energy configuration for each  $x$  value in  $\text{FeGa}_{3-x}\text{Ge}_x$ . Brown, gray and green spheres represents Fe, Ga and Ge atoms respectively. The yellow and blue surfaces represent positive and negative values of the spin density.

on all Fe atoms; (II) in certain configurations it becomes energetically favorable for a few Fe atoms to align antiparallel to their neighbors, indicating the presence of a minor AFM component over the majority FM interaction.

The question then arises on whether all these theoretical predictions can find support on the experimental side. To further investigate the role of Ge doping on the  $\text{FeGa}_3$  crystals, we performed temperature dependent  $^{57}\text{Fe}$  Mössbauer spectroscopy experiments on a single crystal with  $x = 0.27$  Ge doping, which places it far enough into the magnetically ordered ground state region[16] to avoid issues related to non-Fermi-liquid behavior.

Fig. 3(a) shows the Mössbauer spectra for different temperatures between 4.35 and 50 K. From these spectra

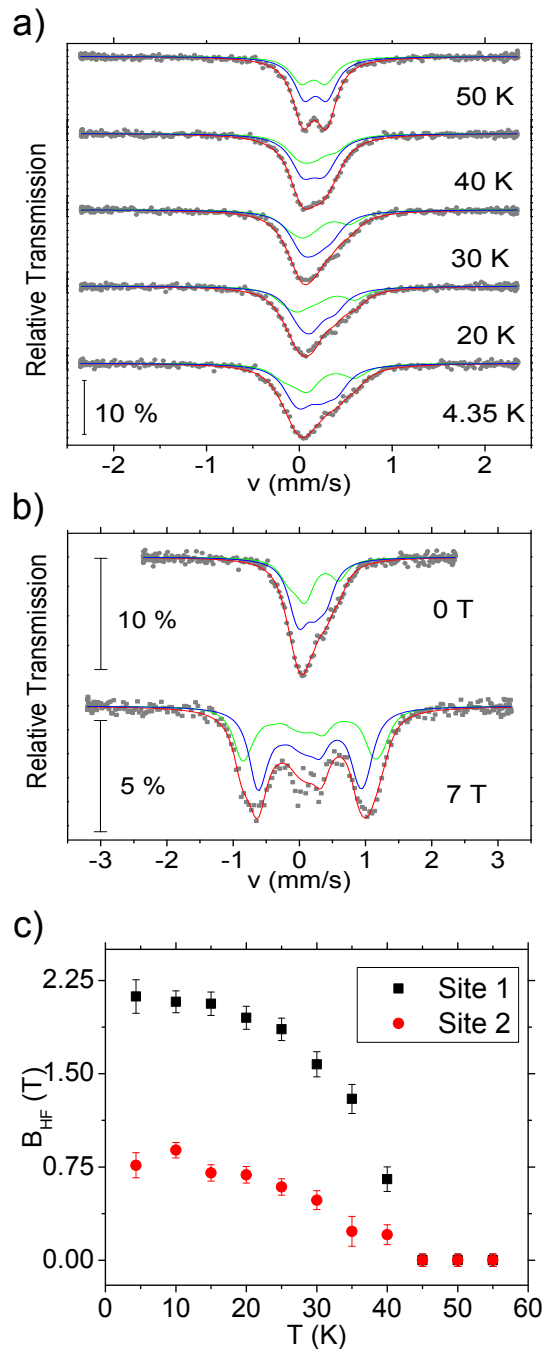


FIG. 3: (a)  $^{57}\text{Fe}$  Mössbauer spectra for temperatures from 4.35 to 50 K. (b)  $^{57}\text{Fe}$  Mössbauer spectra at 4.35 K and zero external field and 7 T external field. (c) Magnetic hyperfine field as a function of temperature within a model with two magnetically inequivalent Fe sites. These parameters were extracted from the spectra in (a).

it is clear that the magnetic order evolves, upon cooling, as a line broadening and a subsequent asymmetric resonance line at low temperatures. We initially attempted to fit these spectra assuming one Fe site (as per the crystal

structure) with a quadrupole interaction as a perturbation of the magnetic interaction between the Fe nucleus and its local environment, within the Full Hamiltonian site analysis. The model fits the data adequately, but the linewidth results are unusually large,  $\sim 0.4$  mm/s. In the Fig. 3(b) we show the 4.35 K Mössbauer spectra for zero field and 7 T external field. Contrary to the zero-field curve, the 7 T spectrum cannot be fitted with a single Fe site, and therefore we re-analyzed all the measured Mössbauer spectra using two magnetically inequivalent Fe sites. The reason this site symmetry breaking is resolved only under external magnetic field is that these two types of Fe atoms can have almost the same electric hyperfine parameters (isomer shift, quadrupole splitting) but different magnetic hyperfine fields (under large external fields the hyperfine field difference is much more evident than at zero field). The requirement of two Fe sites to fit the data must be caused by the Ge substitution on the Ga site, creating different environments for the Fe atom. The magnetic hyperfine fields for the temperature dependent Mössbauer spectra assuming two magnetic sites are shown in the Fig. 3(c). The ratio between the integrated intensities for each site is systematically around 2:3 for all measured spectra.

The Fe site with large magnetic moment ( $0.17 \mu_B/\text{Fe}$  assuming that  $1 \mu_B$  corresponds to a hyperfine field of about 15 T) can be related to a more localized Fe configuration, while the Fe site with smaller magnetic moment ( $\sim 0.08 \mu_B/\text{Fe}$ ) can be related to a Fe site with a more itinerant behavior. The DFT calculations for the lowest energy  $x = 0.25$  configuration result in two magnetic moment distributions around  $0.09 \mu_B/\text{Fe}$  and  $0.38 \mu_B/\text{Fe}$  (see inset of Fig. 1) which agrees quite well with these experimental results.

Finally, we address the issue of an interplay between ferromagnetic vs. antiferromagnetic ground state in the magnetically ordered samples. Fig. 4(a) presents the  $T$ -dependence of the dc magnetic susceptibility of the  $\text{FeGa}_{2.73}\text{Ge}_{0.27}$  crystal under external magnetic fields of  $H = 30$  Oe, 100 Oe and 300 Oe. Fig. 4(b) shows the inverse susceptibility  $(\chi - \chi_0)^{-1} \times T$ , from which a high- $T$  linear fit results in a Curie-Weiss temperature of 53 K, consistent with an effective Ge content  $x = 0.27$ [16]. Upon cooling under the lowest external magnetic field ( $H = 30$  Oe) the magnetization rapidly increases at around 50 K, reaching a sharp maximum and then rapidly decreases between 45–40 K (inset Fig. 4(a)). From there a local minimum is seen and the sample resumes a broad increase until saturating at around 0.487 emu/mol at the lowest measured temperatures. Similar behavior is visible in previous works [16] but not discussed. The small but sharp decrease just below the ferromagnetic ordering temperature evidences a minority of antiferromagnetic interactions present in the sample, resulting in some of the Fe moments aligning antiparallel to the majority, as was found in the DFT calculations

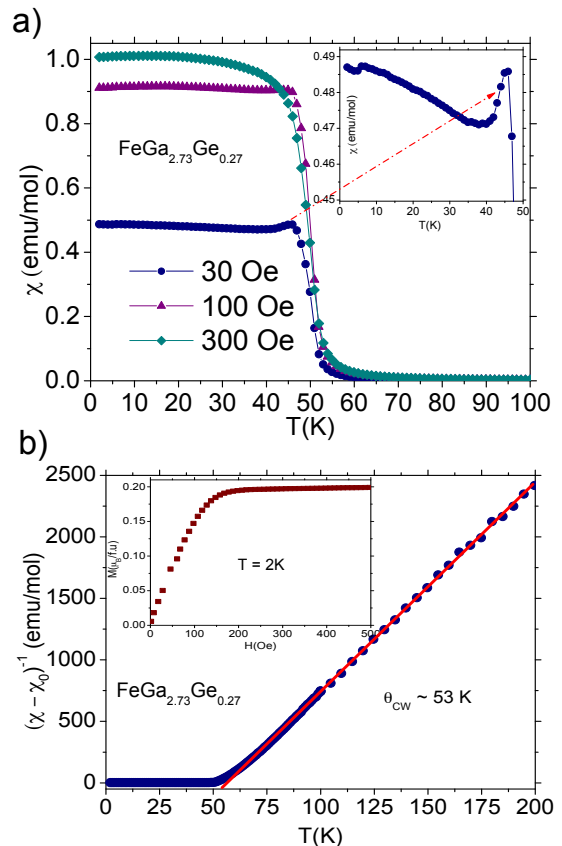


FIG. 4: (a)  $T$ -dependence of the magnetic susceptibility at  $H = 30$  Oe, 100 Oe and 300 Oe. The inset zooms in around the peak region that evidences an anomalous antiferromagnetic behavior. (b) Inverse susceptibility versus temperature.

for  $x = 0.09$  and  $0.19$  lower energy configurations (Figs. 2c and 2e). This is clearly not a trivial case of ferrimagnetism, since the antiparallel moments align themselves at a discernably lower temperature than the majority (possibly indicating a certain level of frustration) and because the antiferromagnetic component proves to be quite fragile. For higher external fields the peak quickly disappears (Fig. 4(a)) and the susceptibility curves adopt a more traditional, monotonic increase upon cooling that is expected of a ferromagnet. This is also supported by low-temperature magnetic isotherms (Fig. 4(b)) where saturation is achieved at only 200 Oe of applied field. In the fully ferromagnetic state, the magnetic moment reaches  $0.18 \mu_B/\text{Fe}$  atom, which is comparable to both the Mössbauer result of  $0.17 \mu_B/\text{Fe}$  and the theoretically calculated average of  $0.22 \mu_B/\text{Fe}$  for the more stable configuration with  $x = 0.25$ , (see Fig. 1).

In conclusion, we have shown that the magnetism of Ge-doped  $\text{FeGa}_3$  is in fact much richer than what had been described so far. Magnetic moment distributions throughout the Fe atoms are complex and strongly de-

pendent on Ge dopant concentration, as well as on the manner in which they are distributed in the lattice. For small dopant concentrations, Fe site symmetry is broken and two different types of Fe atoms emerge: some bearing localized moment (induced by nearby Ge) and the rest remaining non-magnetic. This scenario gradually evolves with increasing Ge concentration to a coexistence of localized and itinerant moments, until a predominantly itinerant magnetism is established at the highest experimentally achieved doping levels ( $x \sim 0.41$ ). Additionally, the magnetic ordering is found to be neither ferromagnetic nor antiferromagnetic, but a combination of majority FM with a minority AFM component brought in by Fe moments that align antiparallel under circumstances not yet fully understood, and once again strongly dependent on the dopant concentration and configuration. All these predictions made by our meticulous DFT calculations were very well supported by Mössbauer and magnetic susceptibility measurements on a  $\text{FeGa}_{2.73}\text{Ge}_{0.27}$  crystal, that showed the existence of two distinct Fe sites having different magnetic moments (despite the single crystallographic site of the  $\text{FeGa}_3$  structure) and a fragile AFM component distinguishable from the major FM transition.

What makes this fascinating system even more compelling is that all these rich features arise even before mixing in the broad range of anomalies accompanying its potential quantum critical behavior around  $x = 0.13$ , which is not contemplated in either the theoretical modeling or the experiments, intentionally performed here on a sample that is well into the magnetically ordered region. Thus, significant progress has been made but much more investigation will be required for proper understanding of all the electronic and magnetic anomalies in doped  $\text{FeGa}_3$ .

This work was supported by Brazilian agencies CAPES, CNPq and FAPESP (Contract #'s 2011/19924-2, 2012/17569-2). JMOG would like to thank CODI-Vicerrectoría de Investigación-Universidad de Antioquia.

- [2] N. Haldolaarachchige, A. B. Karki, W. A. Phelan, Y. M. Xiong, R. Jin, J. Y. Chan, S. Stadler, and D. P. Young, *Journal of Applied Physics* **109** (2011).
- [3] M. Wagner-Reetz, R. Cardoso-Gil, and Y. Grin, *Journal of Electronic Materials* **43**, 1857 (2014).
- [4] J. M. Osorio-Guillén, Y. D. Larrauri-Pizarro, and G. M. Dalpian, *Physical Review B* **86**, 235202 (2012).
- [5] M. Cabrera-Baez, E. T. Magnavita, R. A. Ribeiro, and M. A. Avila, *Journal of Electronic Materials* **43**, 1988 (2013).
- [6] Z. P. Yin and W. E. Pickett, *Phys. Rev. B* **82**, 155202 (2010).
- [7] M. B. Gamża, J. M. Tomczak, C. Brown, a. Puri, G. Kotliar, and M. C. Aronson, *Physical Review B* **89**, 195102 (2014).
- [8] N. Tsujii, H. Yamaoka, M. Matsunami, R. Eguchi, Y. Ishida, Y. Senba, H. Ohashi, S. Shin, T. Furubayashi, H. Abe, et al., *Journal of the Physical Society of Japan* **77**, 1 (2008).
- [9] Y. Hadano, S. Narazu, M. A. Avila, T. Onimaru, and T. Takabatake, *Journal of the Physical Society of Japan* **78**, 3 (2009).
- [10] D. J. Singh, *Physical Review B* **88**, 064422 (2013).
- [11] E. Bittar, C. Capan, G. Seyfarth, P. Pagliuso, and Z. Fisk, *Journal of Physics: Conference Series* **200**, 012014 (2010).
- [12] B. Kotur, V. Babizhetskyy, E. Bauer, F. Kneidinger, A. Danner, L. Leber, and H. Michor, *Materials Science* **49**, 69 (2013).
- [13] A. A. Gippius, V. Y. Verchenko, A. V. Tkachev, N. E. Gervits, C. S. Lue, A. A. Tsirlin, N. Buttgen, W. Kratschmer, M. Baenitz, M. Shatruk, et al., *Physical Review B* **89**, 104426 (2014).
- [14] G. Kresse and J. Furthmüller, *Phys. Rev. B* **54**, 11169 (1996).
- [15] G. Kresse and D. Joubert, *Phys. Rev. B* **59**, 1758 (1999).
- [16] K. Umeo, Y. Hadano, S. Narazu, T. Onimaru, M. A. Avila, and T. Takabatake, *Physical Review B* **86**, 144421 (2012).

---

[1] Y. Amagai, A. Yamamoto, T. Iida, and Y. Takanashi, *Journal of Applied Physics* **96**, 5644 (2004).